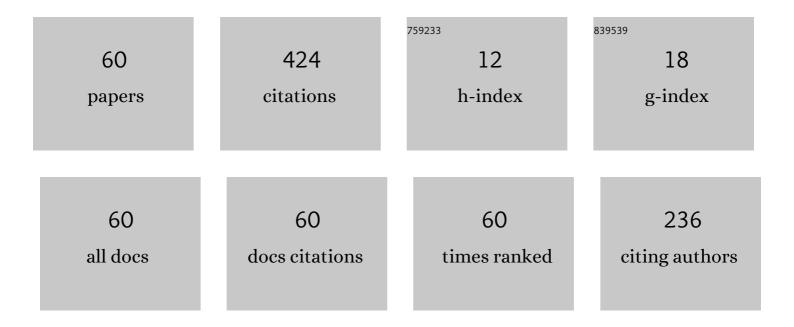
## Maksim Yapryntsev

List of Publications by Year in descending order

Source: https://exaly.com/author-pdf/1816891/publications.pdf Version: 2024-02-01



#	Article	IF	CITATIONS
1	Effect of spark plasma sintering temperature on microstructure and thermoelectric properties of the cermet composites consisting of Bi2Te2.1Se0.9 matrix and Co@CoTe2 inclusions. Journal of Solid State Chemistry, 2022, 305, 122696.	2.9	6
2	Thermoelectric properties of medium-entropy PbSbTeSe alloy prepared by reactive spark plasma sintering. Materials Letters, 2022, 309, 131416.	2.6	7
3	Preparation and characterization of nonstoichiometric Te-deficient and Te-rich thermoelectric Bi2-Gd Te3± compounds. Journal of Alloys and Compounds, 2022, 900, 163516.	5.5	3
4	Features of microstructure and thermoelectric properties of the cermet composites based on grained Bi2Te3 matrix with locally-gradient Ni@NiTe2 inclusions. Chinese Journal of Physics, 2022, 77, 24-35.	3.9	6
5	Interconnected effects of direct Gd doping and accompanying indirect Te-stoichiometry destroying on the thermoelectric properties of Te-rich Bi2-Gd Te3+ compounds. Journal of Solid State Chemistry, 2022, 308, 122945.	2.9	1
6	Microstructure Features of Metal-Matrix Composites Based on Thermoelectric Bismuth Telluride Matrix and Ferromagnetic Filler. Glass and Ceramics (English Translation of Steklo I Keramika), 2022, 78, 442-447.	0.6	8
7	Interconnected effects of Sm-doping on grain structure and transport properties of the textured Bi2-Sm Te2.7Se0.3 compounds. Journal of Solid State Chemistry, 2022, 312, 123176.	2.9	3
8	Synthesis and thermal behavior of Co/AlCe layered double hydroxide. Solid State Sciences, 2021, 111, 106498.	3.2	3
9	Magnetic Materials Based on Layered Double Hydroxides. Petroleum Chemistry, 2021, 61, 388-393.	1.4	0
10	Enhanced thermoelectric efficiency of the bulk composites consisting of "Bi2Te3 matrix―and "filler Ni@NiTe2 inclusions― Scripta Materialia, 2021, 194, 113710.	5.2	11
11	Mixed conductivity analysis of single crystals of <i>α</i> ‴-(Cd1â^' <i>x</i> Zn <i>x</i> )3As2 ( <i>x</i> = 0.45). AlP Advances, 2021, 11, .	1.3	1
12	Effect of Sm-doping on microstructure and thermoelectric properties of textured n-type Bi2Te2.7Se0.3 compound due to change in ionic bonding fraction. Journal of Solid State Chemistry, 2021, 297, 122047.	2.9	7
13	Forming the locally-gradient Ni@NiTe2 domains from initial Ni inclusions embedded into thermoelectric Bi2Te3 matrix. Materials Letters, 2021, 290, 129451.	2.6	9
14	Microstructure evolution and phase transformation of ZrB2-ZrO2-MoSi2-Al coating during annealing treatment. Materials Today: Proceedings, 2021, , .	1.8	1
15	Microstructure and thermoelectric properties of the medium-entropy block-textured BiSbTe1.5Se1.5 alloy. Journal of Alloys and Compounds, 2021, 872, 159743.	5.5	13
16	Kinetics Investigation of the Formation of a Gas-Resistant Glass-Forming Layer during the Oxidation of ZrB2-MoSi2-Y2O3-Al Coatings in the Air Atmosphere. Coatings, 2021, 11, 1018.	2.6	4
17	A Study of the Influence of Irradiation of Carbon Diamond-Like Coatings with Nanosecond Laser Pulses on Their Structural-Phase Composition and Tribological Properties. Russian Physics Journal, 2021, 64, 1055-1059.	0.4	0
18	Oxidation Behavior and Microstructural Evolution of ZrB2–35MoSi2–10Al Composite Coating. Coatings, 2021, 11, 1531.	2.6	2

MAKSIM YAPRYNTSEV

#	Article	IF	CITATIONS
19	Novel cerium-containing layered double hydroxide. Chemical Papers, 2020, 74, 367-370.	2.2	7
20	Thermoelectric properties of the textured Bi1.9Gd0.1Te3 compounds spark-plasma-sintered at various temperatures. Journal of the European Ceramic Society, 2020, 40, 742-750.	5.7	21
21	Measuring current effect on low-temperature resistivity of n-type Bi1.9Lu0.1Te3 compound: Probing the changing in conductivity mechanism under weak electric field. Physica B: Condensed Matter, 2020, 597, 412424.	2.7	0
22	Comparative analysis of the thermoelectric properties of the non-textured and textured Bi1.9Gd0.1Te3 compounds. Journal of Solid State Chemistry, 2020, 290, 121559.	2.9	19
23	Effect of the Synthesis Method on the Phase Composition and Magnetism of Layered Double Hydroxides. Inorganic Materials, 2020, 56, 747-753.	0.8	6
24	Anisotropy of the grain size effect on the electrical resistivity of n-type Bi1.9Gd0.1Te3 thermoelectric textured by spark plasma sintering. Journal of the European Ceramic Society, 2020, 40, 3431-3436.	5.7	7
25	STRUCTURAL-PHASE STATE OF NANOCOMPOSITE ZrB2-MoSi2 COATINGS FOR CARBON/CARBON COMPOSITES DEPOSITED BY A NEW MULTI-CHAMBER DETONATION ACCELERATOR. , 2020, , .		Ο
26	Structural-phase state of near-surface layers of VT6 titanium alloy after femtosecond laser treatment. Letters on Materials, 2020, 10, 243-248.	0.7	0
27	Stabilization of Cerium(III) in the Structure of Hydrotalcite-Like Layered Double Hydroxides. Petroleum Chemistry, 2019, 59, 751-755.	1.4	1
28	Probing the low-temperature magnetic ordering in magnetic ZnMn2As2 semiconductor via transverse magnetoresistance examination. Materials Research Express, 2019, 6, 105908.	1.6	1
29	Synthesis of a Magnetic Core/Shell Nanocomposite Containing Layered Double Hydroxide. Petroleum Chemistry, 2019, 59, 875-879.	1.4	0
30	Cobalt-based ZIF-68 and ZIF-69 as the precursors of non-platinum electrocatalysts for oxygen reduction. Mendeleev Communications, 2019, 29, 544-546.	1.6	5
31	Thermoelectric Properties of Bi2 –xLuxTe2.7Se0.3 Solid Solutions. Semiconductors, 2019, 53, 673-677.	0.5	0
32	Influence of the Sintering Temperature on the Thermoelectric Properties of the Bi1.9Gd0.1Te3 Compound. Semiconductors, 2019, 53, 615-619.	0.5	0
33	Effect of Spark Plasma Sintering Temperature on Thermoelectric Properties of Grained Bi1.9Gd0.1Te3 Compound. Semiconductors, 2019, 53, 1838-1844.	0.5	0
34	Effect of Heat Treatment on the Microstructure and Phase Composition of ZrB2–MoSi2 Coating. Coatings, 2019, 9, 779.	2.6	13
35	Sintering temperature effect on thermoelectric properties and microstructure of the grained Bi1.9Gd0.1Te3 compound. Journal of the European Ceramic Society, 2019, 39, 1193-1205.	5.7	16
36	Transverse magnetoresistance peculiarities of thermoelectric Lu-doped Bi2Te3 compound due to strong electrical disorder. Journal of Rare Earths, 2019, 37, 292-298.	4.8	11

MAKSIM YAPRYNTSEV

#	Article	IF	CITATIONS
37	Effect of BiScO3 Additive on the Structure and Electrical Properties of the Y2O3-ZrO2-SrTiO3 System. Journal of Nano- and Electronic Physics, 2019, 11, 01018-1-01018-4.	0.5	3
38	Nanostructured Coatings Based on Amorphous Carbon and Gold Nanoparticles Obtained by the Pulsed Vacuum-arc Method. Journal of Nano- and Electronic Physics, 2019, 11, 04019-1-04019-7.	0.5	1
39	Variable-range hopping conductivity in Lu-doped Bi2Te3. Solid State Sciences, 2018, 76, 111-117.	3.2	15
40	Mechanisms of thermoelectric efficiency enhancement in Lu-doped Bi <sub>2</sub> Te <sub>3</sub> . Materials Research Express, 2018, 5, 015905.	1.6	24
41	Preparation of crystalline Mg(OH)2 nanopowder from serpentinite mineral. International Journal of Mining Science and Technology, 2018, 28, 499-503.	10.3	27
42	Effects of Lu and Tm Doping on Thermoelectric Properties of Bi2Te3 Compound. Journal of Electronic Materials, 2018, 47, 1362-1370.	2.2	29
43	Microstructure and thermoelectric properties of Bi1.9Lu0.1Te3 compound. Rare Metals, 2018, 37, 642-649.	7.1	4
44	Enhancement of thermoelectric efficiency in Bi2Te3 via rare earth element doping. Scripta Materialia, 2018, 146, 91-94.	5.2	49
45	Asymmetry and Parity Violation in Magnetoresistance of Magnetic Diluted Dirac–Weyl Semimetal (Cd <sub>0.6</sub> Zn <sub>0.36</sub> Mn <sub>0.04</sub> ) <sub>3</sub> As <sub>2</sub> . Physica Status Solidi - Rapid Research Letters, 2018, 12, 1800386.	2.4	8
46	Electric field effect on variable-range hopping conductivity in Bi1.9Lu0.1Te3. Physica B: Condensed Matter, 2018, 545, 222-227.	2.7	7
47	Anisotropic thermoelectric properties of Bi1.9Lu0.1Te2.7Se0.3 textured via spark plasma sintering. Solid State Sciences, 2018, 84, 28-43.	3.2	25
48	Specific features of the transport properties of the Lu0.1Bi1.9Te3 compound. Semiconductors, 2017, 51, 989-991.	0.5	0
49	Synthesis and electrical properties of Bi2Te3-based thermoelectric materials doped with Er, Tm, Yb, and Lu. Semiconductors, 2017, 51, 710-713.	0.5	3
50	Fracture toughness of Al <sub>2</sub> O <sub>3</sub> /ZrSiO <sub>4</sub> coatings obtained by multi-chamber gas-dynamic accelerator. Journal of Physics: Conference Series, 2017, 857, 012001.	0.4	1
51	Zircon-Based Ceramic Coatings Formed by a New Multi-Chamber Gas-Dynamic Accelerator. Coatings, 2017, 7, 142.	2.6	15
52	Manufacture, Structure, and Electric Conductivity of ZrO2–SrTiO3–BiScO3 Ceramics. Glass and Ceramics (English Translation of Steklo I Keramika), 2016, 72, 413-416.	0.6	1
53	MICROSTRUCTURE AND MECHANICAL PROPERTIES OF ALUMINA POWDER COATINGS BY A NEW MULTI-CHAMBER DETONATION SPRAYER. Surface Review and Letters, 2016, 23, 1550088.	1.1	2
54	Deposition of Alumina-titania Nanostructured Coating by a New Multi-chamber Gas-dynamic Accelerator. Journal of Nano- and Electronic Physics, 2016, 8, 03018-1-03018-4.	0.5	0

MAKSIM YAPRYNTSEV

#	Article	IF	CITATIONS
55	Linear Positive Magnetoresistivity of the Bi1.9Lu0.1Te3 Alloy with Inhomogeneous Micrograined Structure. Journal of Nano- and Electronic Physics, 2016, 8, 04033-1-04033-4.	0.5	Ο
56	Low-temperature Minimum in the Electrical Resistivity of the Bi1.9Lu0.1Te3. Journal of Nano- and Electronic Physics, 2016, 8, 04036-1-04036-4.	0.5	0
57	Deposition and Characterization of the Titanium-Based Coating by a Multi-Chamber Detonation Sprayer. MATEC Web of Conferences, 2015, 30, 01008.	0.2	Ο
58	Structure and Properties of the Hardmetal Coatings Cr3C2-25NiCr Formed by a Multi-chamber Detonation Sprayer. MATEC Web of Conferences, 2015, 30, 01009.	0.2	1
59	Effect of Heat Treatment of the Alumina Powder on the Microstructure and Properties of Coatings. MATEC Web of Conferences, 2015, 30, 01003.	0.2	Ο
60	Effect of processing parameters on the microstructure and properties of WC–10Co–4Cr coatings formed by a new multi-chamber gas-dynamic accelerator. Ceramics International, 2015, 41, 15067-15074.	4.8	17